

## A NOVEL APPROACH TO SYNTHESIS AND CHARACTERIZATION OF TITANIUM DIOXIDE NANOPARTICLES FOR PHOTOCATALYTIC APPLICATIONS

K. MANIKANDAN<sup>a\*</sup>, A. J. AHAMED<sup>b</sup>, A. THIRUGNANASUNDAR<sup>c</sup>,  
G. M. BRAHMANANDHAN<sup>d</sup>

<sup>a</sup>*Department of Chemistry, Velalar College of Engineering and Technology,  
Erode-638 012, India.*

<sup>b</sup>*PG and Research Department of Chemistry, Jamal Mohamed College  
(Autonomous), Trichy-620 020, India*

<sup>c</sup>*Department of Chemistry, Velalar College of Engineering and Technology,  
Erode-638012, India*

<sup>d</sup>*Department of Nuclear Science and Engineering, SRM University,  
Kattankulathur- 603 203, India*

This paper presents synthesis of titanium dioxide nanoparticles by solgel method using titanium (IV) isopropoxide. The method is simple and easy to reproduce. Structural and micro structural characterizations of TiO<sub>2</sub> nanoparticles were carried out using X-ray diffraction (XRD), Scanning Electron Microscopy (SEM) techniques. The particles of synthesized TiO<sub>2</sub> shows anatase nature crystal structure, when calcined at 500°C and 600°C for 5 hours, but when calcined at 700°C they undergo structural changes to rutile structure at the same duration of calcination. XRD calculations of TiO<sub>2</sub> prepared by solgel method showed particle size from 30 to 47nm. Elemental analysis was done by energy dispersive X-ray atomic spectrum. TiO<sub>2</sub> nano particles were further characterised by UV-Visible spectroscopy and photoluminescence study. From the UV-Visible analysis, it has been revealed that when calcinations temperature increases, the band gap decreases from 3.1 to 2.85eV. The luminescence property of the TiO<sub>2</sub> nanoparticles was analysed by the photoluminescence spectrum, which confirmed that direct recombination between electrons in the conduction band and holes in the valence band. The photocatalytic activity of synthesized TiO<sub>2</sub> nanoparticles has been investigated using methylene blue dye as model dye. The irradiation time of the TiO<sub>2</sub> nanoparticles prepared by sol-gel method were taken into account for the photocatalytic degradation process.

(Received September 22, 2015; Accepted December 19, 2015)

*Keywords:* TiO<sub>2</sub>, Solgel method, XRD, SEM, Particle size, Photo catalyst

### 1. Introduction

TiO<sub>2</sub> is also known as Titania, and it is a naturally occurring oxide of Titanium. The light absorption, high refractive index, non-toxic property, chemically high stable are some of the properties of Titanium dioxide and it has relatively low-cost production [1-5]. Titanium dioxide has been widely used in paints as a pigment and filler [6], ointments, toothpaste etc [7-9]. Particles of Titanium dioxide have important role in the fields of photo catalyst material for degradation of organic contaminants [10], environmental purification, sensors and photo-electric chemical conversions in solar cells [11], electronic devices, photo electrodes and gas sensors. The performance of TiO<sub>2</sub> is strongly depends on size, the crystalline structure, and the morphology of the particles [12–15]. The shape, crystal structure and size of TiO<sub>2</sub> do not only vary with surface stability changes, but also the transitions take place between various phases of TiO<sub>2</sub> under heat and

---

\*Corresponding author: chem\_mani03@yahoo.co.in

pressure. Normally  $\text{TiO}_2$  exist in three forms, Rutile (Tetragonal,  $a=b=3.78\text{\AA}$ ,  $c=9.5\text{\AA}$ ), Anatase (Tetragonal,  $a=b=3.78\text{\AA}$ ,  $c=9.5\text{\AA}$ ) and Brookite (Rhombohedral,  $a=5.43\text{\AA}$ ,  $b=9.16\text{\AA}$ ,  $c=5.13\text{\AA}$ ) forms. These all crystalline forms consist of  $[\text{TiO}_6]^{2-}$  octahedral structure. Anatase form of  $\text{TiO}_2$  has a wider optical band gap (3.2 eV), a higher fermi level, a smaller electron effective mass, and high mobility of charge carriers. But Rutile phase is highly stable phase at high temperature [16]. The edges and corners of this structure have different manners, but the overall stoichiometry as  $\text{TiO}_2$  [17, 18]. Transformation of Anatase-to-Rutile is usually occurs at 600 to 700°C [19-21]. Phase transition to Rutile is non-reversible. Because, Rutile form has greater thermodynamic stability compared to anatase phase [22, 23]. So there has been a variety of researchers focusing the preparation of nanoparticles of  $\text{TiO}_2$  using Ethanol along with different acid and bases, for various applications. Hence a novel approach, in this paper, an easy way of synthesizing nano particles of  $\text{TiO}_2$  using Titanium (IV) Isopropoxide Ethanol and hydroxylamine hydrochloride has been discussed.

## 2. Materials and methods

Aqueous solution of Titanium (IV) Isopropoxide (purity >99.9%) analar grade (Sigma-Aldrich) was used as starting material. Solgel is the most simple and sophisticated method proposed by Byun et.al, [24] among the various methods for producing nanoparticles. Titanium isopropoxide is used as starting material. The sol was prepared by mixing Titanium isopropoxide (3ml) with 24 ml of Ethanol and dissolved 1000ml of deionised water at room temperature. The molar ratio of Titanium isopropoxide is 1:8 respectively. Hydroxylamine hydrochloride 0.694gms was dissolved in 100ml of deionised water and added gradually to the Titanium isopropoxide sol. After 30 minutes of vigorous stirring the suspension was centrifuged and precipitate obtained was washed with single step deionised water. After centrifugation the precipitate was dried at 105°C till the samples were converted into dry powder. The prepared samples were calcined at 500°C, 600°C and 700°C for five hour at a constant temperature rise of 2°C/minute.

X-ray diffraction pattern analysis for pure  $\text{TiO}_2$  nanoparticles was recorded by LabX XRD6000 Shimadzu model with Cu-K $\alpha$  radiation. The structure and morphology of the nanoparticles were investigated by Scanning Electron Microscope (SEM) using Jeol JSM 6390 Scanning Microscope. The absorption spectra and optical band gap of the  $\text{TiO}_2$  nanoparticle samples were measured by using UV-Vis spectrophotometer (JASCO U-670 Spectrometer). The photoluminescence analysis was carried out by using Horiba Jobnyvon.

## 3. Results and discussion

### 3.1. X-Ray Diffraction Analysis (XRD)

Figs. 1, 2 and 3 show the XRD patterns of  $\text{TiO}_2$  prepared by solgel method calcined at 500°C, 600°C and 700°C respectively. From the XRD pattern it is clear that the  $\text{TiO}_2$  is in its Anatase form when it is calcined at 500°C, 600°C. Phase transformation to Rutile form is identified in XRD results when calcination temperature increased to 700°C. The obtained  $2\theta$  values and corresponding (hkl) planes are 25.3°(101), 38°(004), 48°(200), 54°(105), 63°(204), 69.23°(116), 70.89°(220), 75.38°(215) respectively for  $\text{TiO}_2$  samples calcined at 500°C, 600°C (JCPDS Card No.21-1272). When calcination temperature increases to 700°C, shows the slight shifting of peaks at 27.3°, 36°, 41.2°, 54°, 69° (in figure 3) corresponding to the hkl values (110), (101), (111), (210), (112) (JCPDS Card No.88-1175) indicate that phase has been changed from Anatase into Rutile. The preferred peak for  $2\theta$  value 25.3° was observed with corresponding plane (101), which is the strongest peak among other peaks for all the  $\text{TiO}_2$  nanoparticles calcined at temperatures of 500°C, 600°C which is not available when the calcination temperature increased to 700°C, supports the changes in phase from Anatase to Rutile. The peaks of the graph are in good agreement with the literature report by Akarsu et al [25]. The average size of the particles was calculated using Debye-Scherrer's formula. Crystallite size =  $0.9\lambda/\beta\cos\theta$ , where  $\beta$  is the full

width at half-maximum ( $\text{FWHM}_{\text{hkl}}$ ) of an hkl peak at  $2\theta$  value,  $\theta$  is the half of the scattering angle. From the formula, the calculated particle sizes are given in Table-1

Table 1: Crystallite size of synthesized  $\text{TiO}_2$  by solgel method at different calcined temperatures

S.No	$\text{TiO}_2$ synthesized by solgel method	Crystallite size(nm)
1	Calcined at $500^\circ\text{C}$	30nm
2	Calcined at $600^\circ\text{C}$	27nm
3	Calcined at $700^\circ\text{C}$	47nm

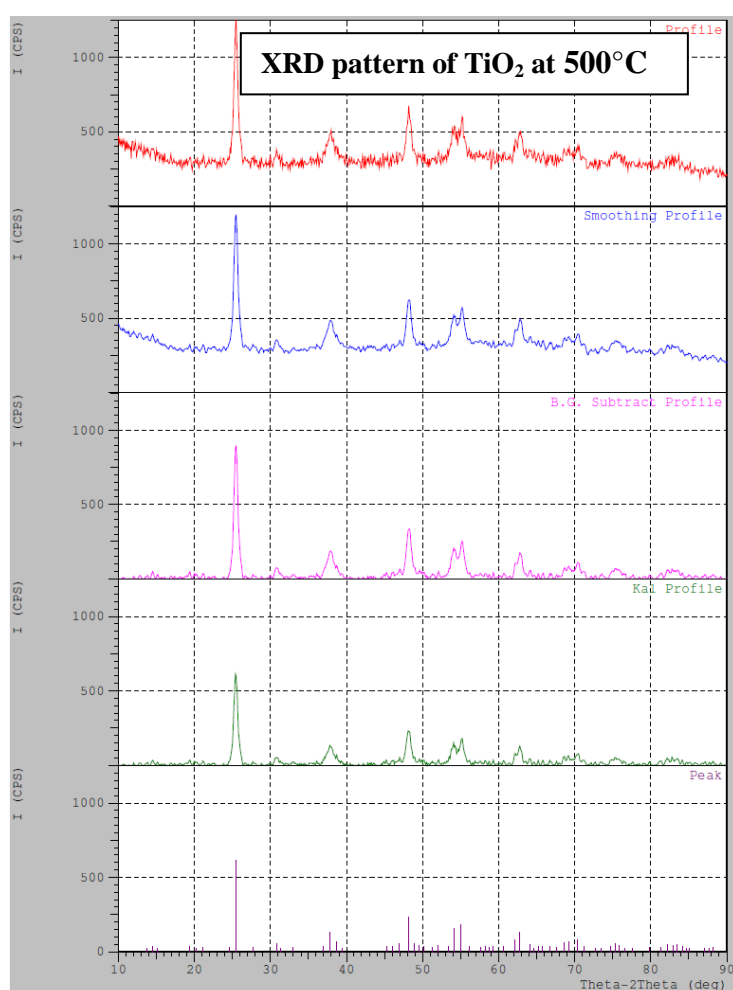


Fig. 1. XRD pattern of  $\text{TiO}_2$  at  $500^\circ\text{C}$

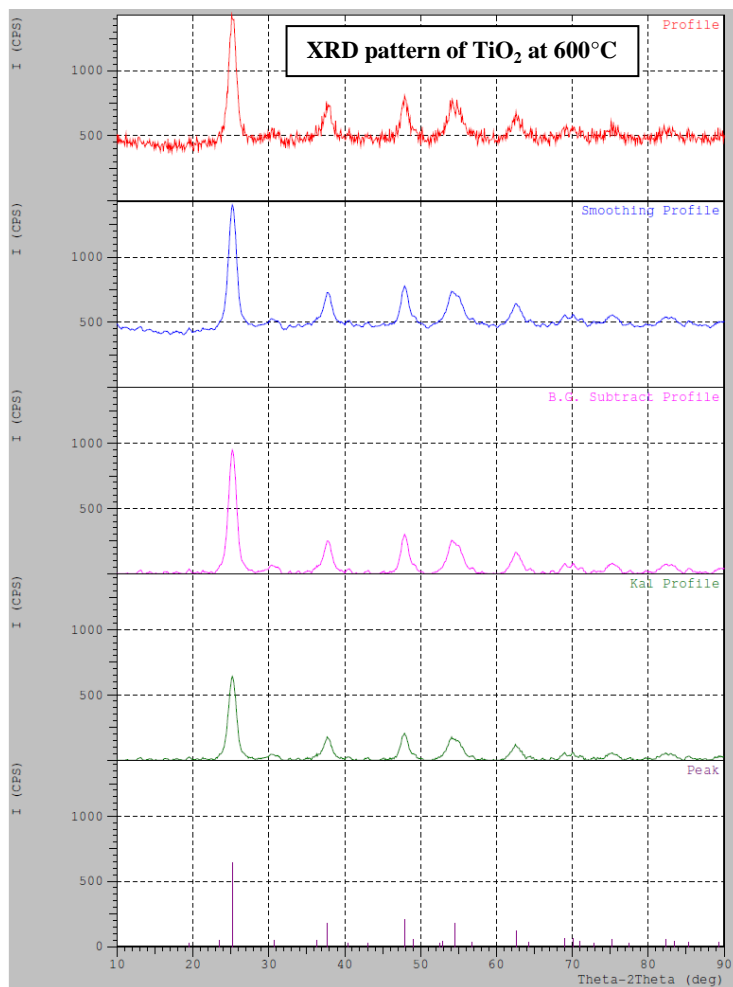


Fig. 2: XRD pattern of  $\text{TiO}_2$  at  $600^\circ\text{C}$

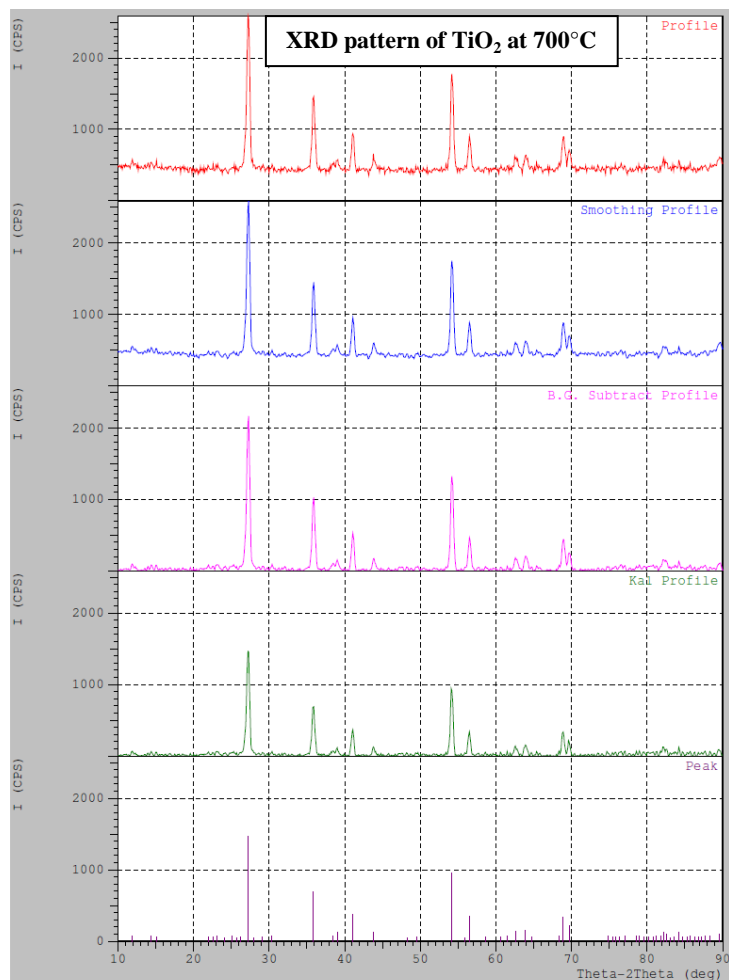


Fig. 3: XRD pattern of TiO<sub>2</sub> at 700°C

### 3.2. Scanning Electron Microscope

The images of TiO<sub>2</sub> nanoparticles under Scanning Electron Microscope are shown in Fig. 4, 5 and 6. From the images, it has been confirmed that the grains of nanoparticles of TiO<sub>2</sub> appear to be nearly spherical and uniform sized particles and coherent together. However, the individual spherical particles are not clearly seen due to the nano-clusters formed during the growth.

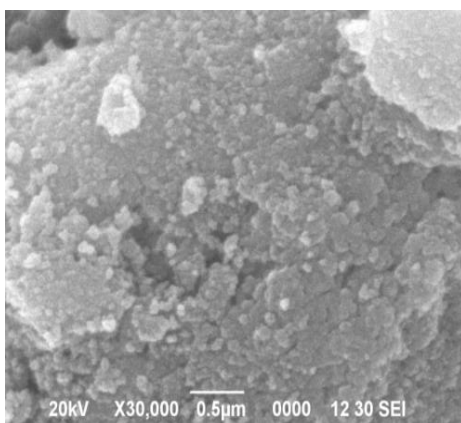
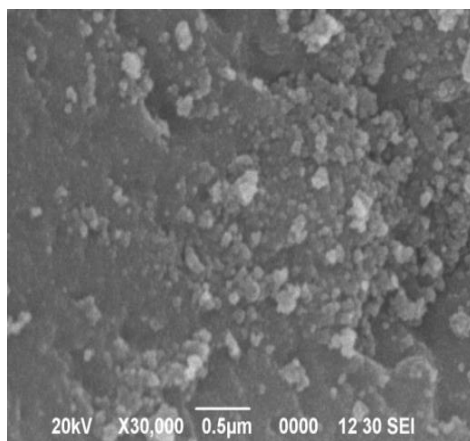
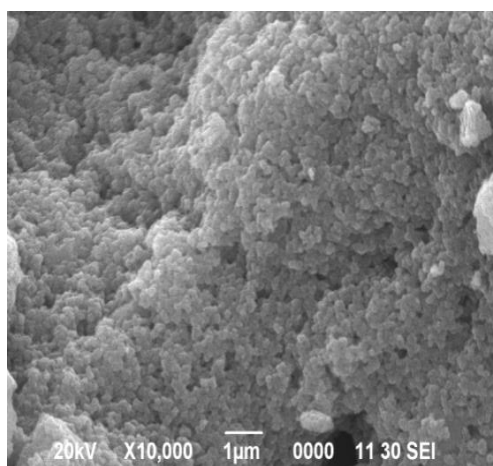


Fig. 4. Scanning Electron Microscope image of TiO<sub>2</sub> prepared by sol gel method calcined at 500°C



*Fig. 5. Scanning Electron Microscope image of TiO<sub>2</sub> prepared by sol gel method calcined at 600°C*



*Fig. 6. Scanning Electron Microscope image of TiO<sub>2</sub> prepared by sol gel method calcined at 700°C*

### **3.3. Energy Dispersive Analysis by X-rays (EDX)**

EDXA is used to analyze the chemical composition of a material. Figure 7 represents the EDXA of TiO<sub>2</sub> nanoparticles prepared by solgel method. EDXA shows only peaks of titanium and oxygen. From figure 7, it is clear that TiO<sub>2</sub> is free from impurities. The same results were reproduced for all the synthesized TiO<sub>2</sub> samples.

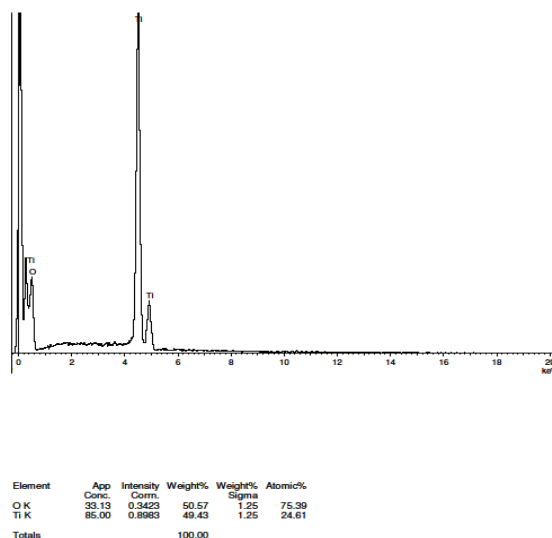


Fig. 7: EDXA Analysis of  $\text{TiO}_2$  prepared by solgel method.

### 3.4. UV-VIS analysis of $\text{TiO}_2$ nanoparticles

UV-Visible spectroscopy measurement has been performed to measure the absorbance and band gap for  $\text{TiO}_2$  nanoparticles. The optical absorbance spectra of  $\text{TiO}_2$  nanoparticle at 500, 600 and 700°C are shown in figure 8. The absorption spectra of all  $\text{TiO}_2$  samples exhibit strong absorption below 400nm. The UV-Visible spectrum of  $\text{TiO}_2$  nanoparticle samples at 500, 600 and 700°C indicates the absorption peaks at around 346nm, 349nm and 345nm.

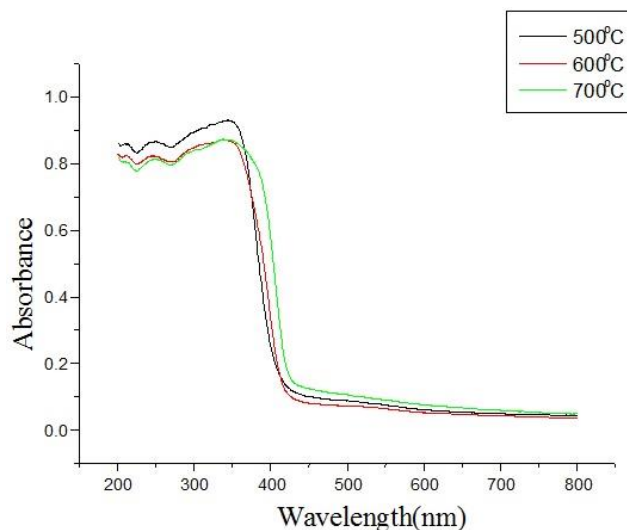


Fig 8. UV-Vis absorbance spectra of  $\text{TiO}_2$  samples calcined at (a) 500°C (b) 600°C (c) 700°C

The direct band gap ( $E_g$ ) of the samples is determined by fitting the absorption data to the direct transition

$$Ah\nu = E_d(h\nu - E_g)^{1/2}$$

Where  $\alpha$  is the optical absorption coefficient,  $h\nu$  is the photon energy,  $E_g$  is the direct band gap, and  $E_d$  is a constant [26]. The band gap, ( $E_g$ ), of  $\text{TiO}_2$  can be measured by graph drawn between  $(\alpha/h\nu)^2$  against photon energy, and extrapolation the linear portion of the curve to absorption equal to zero as given in figure 9 (also called a Tauc plot) [27,28].

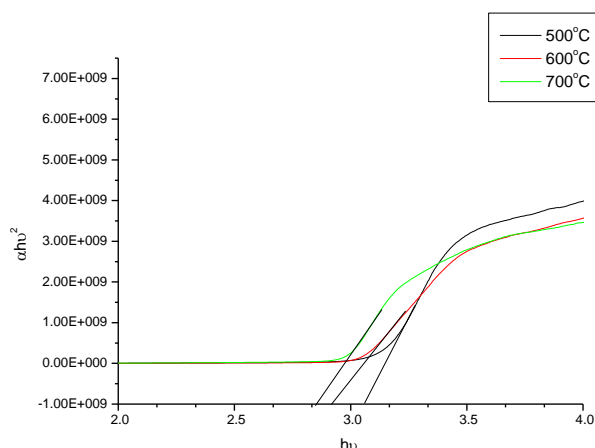


Fig. 9: UV-Vis absorbance spectra and band gap of  $\text{TiO}_2$  samples calcined at (a)  $500^\circ\text{C}$  (b)  $600^\circ\text{C}$  (c)  $700^\circ\text{C}$

The UV Visible spectrum of  $\text{TiO}_2$  nanoparticle samples at 500, 600 and  $700^\circ\text{C}$  indicate the absorption at around 346 nm, 349nm and 345nm in UV region. The spectrum of  $\text{TiO}_2$  nanoparticle at 500and  $600^\circ\text{C}$  shows the good agreement with band gap of Anatase phase [29]. When the calcination temperature increases, the band gap gradually decreased from 3.1 to 2.85eV. At high calcined temperature of  $700^\circ\text{C}$ , the band gap was at the lowest value (2.850eV), smaller crystallite size have larger band gap [30]. This range of band gap for  $\text{TiO}_2$  nano particles confirms that the formation of  $\text{TiO}_2$  nano particles are in Anatase form at annealing temp 500and  $600^\circ\text{C}$ [29]. This gives good agreement with XRD particle size determination of  $\text{TiO}_2$  nanoparticle samples prepared by solgel method.

### 3.5. Photoluminescence (PL) study

The photoluminescence spectrum has been recorded for  $\text{TiO}_2$  nanoparticles prepared by solgel method and it is shown in figure 10. The emission of first peak in the photoluminescence spectra obtained for three temperatures of calcinations of  $\text{TiO}_2$  nanoparticles between 360 to 385nm corresponds to the direct recombination between electrons in the conduction band and holes in the valence band [31]. Similar peak has been observed in earlier work on  $\text{TiO}_2$  nano particles [32]. The presence of broad peak in the visible region of PL spectrum indicates the presence of defect levels below the conduction band and the electronic transition takes place by defect levels such as oxygen vacancies in the band gap [33].



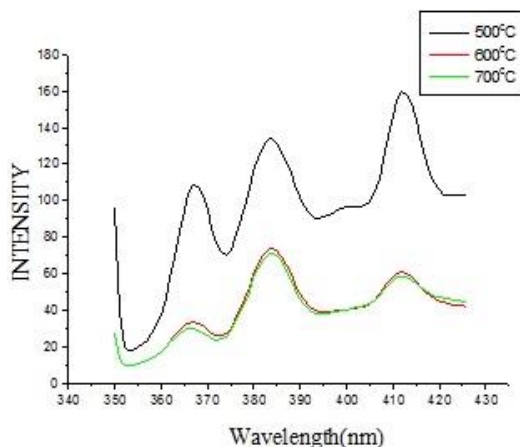


Fig.10: Photoluminescence spectra of  $\text{TiO}_2$  samples calcined at (a)  $500^\circ\text{C}$  (b)  $600^\circ\text{C}$  (c)  $700^\circ\text{C}$

### 3.6. Photocatalysis Decolorisation of Methylene blue on $\text{TiO}_2$ nanoparticles

The Photocatalytic activity of  $\text{TiO}_2$  nanoparticles were investigated using Methylene blue as a model dye and UV irradiation.  $\text{TiO}_2$  nanoparticles prepared by solgel method calcined at  $600^\circ\text{C}$  has taken for this analysis. Fig. 11 and 12 shows efficiency of decolorisation, with the effect of concentration of the dye in presence and absence of  $\text{TiO}_2$  nanoparticles. The decolorisation proceeds slowly in the early stages of irradiation and very fast thereafter. The decolourisation also takesplace very slowly in the absence of the catalyst  $\text{TiO}_2$ . This is consistent with the observations of Kuo and Ho[34].

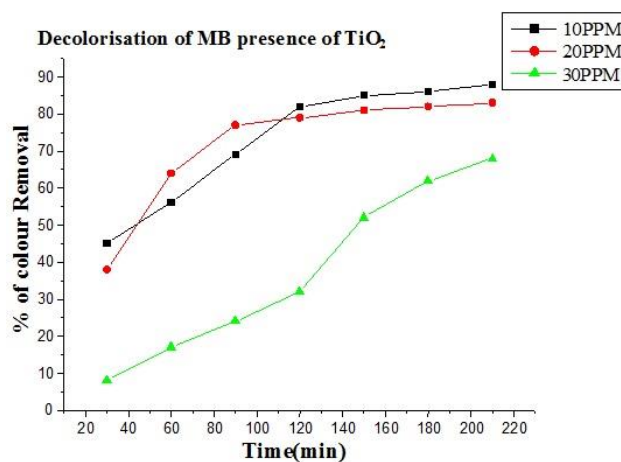


Fig.11. Effect of Concentration of Methylene Blue on the efficiency of decolourisation in UV in presence of  $\text{TiO}_2$

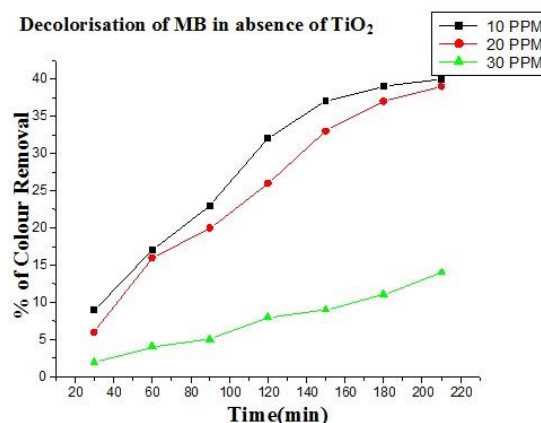
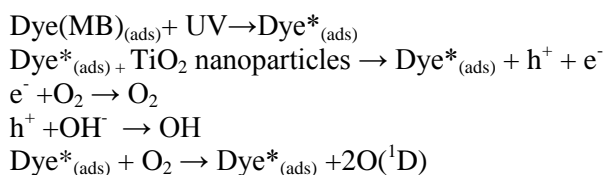


Fig. 12. Effect of Concentration of Methylene Blue on the efficiency of decolourisation in UV in absence of  $\text{TiO}_2$

It is seen that, under UV irradiation, the colour removal efficiency in terms of percentage of the initial dye concentration decreased with increase in the initial concentration of the dye, presence of the catalyst. At higher concentration of the dye, the path of photon entering the solution decreases and at low concentration the reverse effect is observed higher concentrations lead to a reduction in the light penetration and thus reduction in the exposure of catalyst surface.



#### 4. Conclusion

Titanium dioxide nanoparticles have been successfully synthesised with using of Hydroxylamine Hydrochloride as a hydrolysis catalyst. Anatase  $\text{TiO}_2$  is obtained by solgel method when calcined at  $500^\circ\text{C}$  and  $600^\circ\text{C}$  for 5 hours.  $\text{TiO}_2$  prepared by solgel method is converted to Rutile form when it is calcined at  $700^\circ\text{C}$  for 5 hours.  $\text{TiO}_2$  nano particle size determined from X-ray diffraction analysis is 30 nm, 27nm and 47nm. EDXA analysis shows that no impurities are present in the prepared  $\text{TiO}_2$  samples. UV-Visible spectrum of  $\text{TiO}_2$  nanoparticles at three temperatures indicates strong absorption in the region of 346 nm, 349nm and 345nm for 500, 600 and  $700^\circ\text{C}$ . The band gaps of nano $\text{TiO}_2$  measured by graphical method are 3.10ev, 2.90ev and 2.85eV. Photoluminescence study indicates that the strong emission peaks obtained in 383nm, 385nm and 385nm region confirm direct recombination between electrons in the conduction band and holes in the valence band. From the results, is it clear that, the prepared  $\text{TiO}_2$  particles are nano-sized and possess Anatase and Rutile phase. The decolourisation of Methylene Blue takesplace slowly in the initial stages of photocatalytic reaction and increases thereafter in the presence of the catalyst  $\text{TiO}_2$ . But decolourisation takeplace very slowly in the earlier stage of photo catalytic reaction and slightly increases in the absence of  $\text{TiO}_2$ .

#### References

- [1] P.V. Kamat, Photochemistry on nonreactive and reactive (semiconductor) surfaces, Chemical Review, **93**(1),267 (1999).
- [2] A.Rammal, F.Brisach, M.Henry, C.R.Chimie, Comptes Rendus Chimie, **5**(1),59 (2002).

- [3] Rubing Zhang, Lian Gao, Qinghong Zhang, *Chemosphere*, **54**(3),405(2004).
- [4] P.S.Awati, S.V.Awate, P.P.Shah, V.Ramaswamy, *Catalysis communications*, **4**(8),393 (2003).
- [5] Andrew Mills, George Hill, Sharan Bhopal, Ivan P. Parkin, Shane A. O'Neill, *Journal of Photochemistry and Photobiology A: Chemistry*, **160**(3),185(2003).
- [6] Krishnamurthy Prasad, D.V. Pinjari, A.B. Pandit, S.T. Mhaske, *Ultrasonics Sonochemistry*, **17**(2),409 (2010).
- [7] Shuai Yuan, Wanhua Chen, Shengshui Hu, *Fabrication Material Science Engineering C*, **25**(4),479(2005).
- [8] H.Juergen, Braun, Andrejs Baidins, Robert E. Marganski, *Progress in Organic Coatings*, **20**(2),105(1992).
- [9] R.Zallen, M.P.Moret, *Solid state Communications*, **137**(3),154 (2006).
- [10] Desong Wang, Libin Xiao, Qingzhi Luo, Xueyan Li, Jing An, Yandong Duan, *Journal of Hazardous Materials*, **192**(1),150 (2011).
- [11] M. Alam Khan, M. Shaheer Akhtar, O-Bong Yang, *Solar energy*,**84**(12),2195 (2010).
- [12] L.Kavan, M.Gratzel, S.E.Gilbert, C.Klemenz, H.Scheel, *Journal of American Chemical Society*. **118**(28),6716 (1996).
- [13] R.Krol, A.Goossens, J.Schoonman, Mott-Schottky, *Journal of Electrochemical Society*, **144**(5),1723 (1997).
- [14] G.C.Hadjipanayis, R.W.Siegel, eds., *Nanophase Materials*, Kluwer Academic Publishers, Dordrecht, NATO ASI Series, 1994, pp.E 260.
- [15] R.I.Bickley, T.Gonzalez-Carreno, J.S. Lees, L.Palmisano, R.J.D.Tilley, *Journal of Solid State Chemistry*, **92**(1),178 (1991).
- [16] K. Mogyorosi, I. Dekany, J. H. Fendler, *Langmuir*. **19**(7),2938 (2003).
- [17] H.F.Mark, D.F.Othmer, C.G.Overberger, G.T.Seaberg (Eds), *Encyclopedia of Chemical Technology*, John Wiley, New York, 1983, pp.139.
- [18] R.Weast, *C Hand book of Chemistry and Physics*, CRC Press Boca Raton FL, 1984, pp.B- 54.
- [19] W. Czanderna, C. N. Ramachandra Rao, J. M. Honig, *Transactions of the Faraday Society*, **54**, 1069(1958).
- [20] S.R.Yoganarasimhan, C.N.R.Rao, *Transactions of the Faraday Society*, **58**,1579 (1962).
- [21] S Rajesh Kumar, Suresh C Pillai, U.S Hareesh, P Mukundan, K.G.K Warriar, *Materials letters*,**43**(5-6),286 (2000).
- [22] D.J. Reidy, J.D. Holmes, M.A. Morris, *Journal of the European ceramic society*, **26**(9),1527(2006).
- [23] A.Navrotsky, O.J.Kleppla, *Journal of the American Ceramic Society*, **50**(11) 626-30.
- [24] D.Byun, Y.Kim, K.Lee, P.Hofmann, *Journal of Hazardous Materials*, **73**(2),199 (2000).
- [25] Murat Akarsu, Meltem Asilturk, Funda Sayilkan, Nadir Kiraz, Ertugrul Arpac, Hikmet Sayilk, , *Turkish Journal of Chemistry*, **30**(3),333 (2006).
- [26] E. Ziegler, A. Heinrich, H. Oppermann, G. Stover, *Physica Status Solidi A*, **66**(2),635 (1981).
- [27] J.Tauc, R. Grigorovici, A. Vancu, *Physica Status Solidi B*,**15**(2),627 (1966).
- [28] J. Tauc, *Material Research Bulletin*,**3**(1),37 (1968).
- [29] Z. Ambrus, N. Balazs, T. Alapi, G. Wittmann, P. Sipos, A. Dombi, K.Mogyorosi, *Applied Catalysis B: Environmental*,**81**(1-2),27 (2008).
- [30] P. Dennis Christy, N. S. Nirmala Jothi, N. Melikechi, P. Sagayaraj, *Crystal Research and Technology*, **44**(5), 484 (2009).
- [31] J. Liqiang, S.Xianojun, X.Baiqi, C.Weimin and F.Honggang, *Journal of Solid State Chemistry*, **177**,3375 (2004).
- [32] R.Vjayalakshmi, V.Rajendran, *Archives of Applied Science Research*, **4**(2),1183 (2012).
- [33] Y. Zhao, C.Z. Li, X. H. Liu, F. Gu, H. B. Jiang, W. Shao, L. Zhang, Y. He, *Material Letter*, **61**, 79 (2007).
- [34] W.S.Kou, P.H.Ho, *Solar photocatalytic decolorization of methylene blue in water*, *Chemosphere* **45**, 77 (2001).